Earth Planets Space, **59**, 1073–1082, 2007

Interseismic deformation of the Nankai subduction zone, southwest Japan, inferred from three-dimensional crustal velocity fields

Takao Tabei[1], Mari Adachi[1], Shin'ichi Miyazaki[2], Tsuyoshi Watanabe[3], and Sayomasa Kato[4]

[1]*Department of Natural Environmental Science, Kochi University, Akebono-cho 2-5-1, Kochi 780-8520, Japan*
[2]*Earthquake Research Institute, the University of Tokyo, Yayoi 1-1-1, Bunkyo-ku, Tokyo 113-0032, Japan*
[3]*Graduate School of Environmental Studies, Nagoya University, Furo-cho, Chikusa-ku, Nagoya 464-8602, Japan*
[4]*Shikoku Research Institute Inc., Yashima-nishimachi 2109, Takamatsu 761-0192, Japan*

(Received December 27, 2006; Revised July 10, 2007; Accepted August 28, 2007; Online published October 19, 2007)

We have studied crustal deformation in the Nankai subduction zone, southwest Japan, based on three-dimensional GPS velocity fields. Oblique subduction of the Philippine Sea plate has caused two different modes of deformation of the overriding plate: interseismic crustal shortening in the direction of plate convergence, and permanent lateral movement of the forearc. The block boundary dividing the forearc is the Median Tectonic Line (MTL); however, we assumed that its shallower portion is fully or partially locked to a certain depth. The plate boundary and the MTL are represented by many rectangular faults. We carried out inversion analyses with *a priori* information to estimate simultaneously slip deficit rates at those rectangular faults, together with the rate of lateral movement of the forearc. The results show that the seismogenic subduction faults at a depth of 5–25 km are strongly locked. As for the transition zone at 25–35 km, the inversion analysis results in stronger locking than shown in previous studies, especially when the vertical velocity data are weighted. The rates of lateral forearc movement and slip deficit at the MTL are nearly comparable but in a reverse sense to each other. This shows that the shallower portion of the MTL is strongly locked but that stationary aseismic slip is occurring in the deeper part.

Key words: Crustal deformation, southwest Japan, Nankai Trough, Median Tectonic Line, Global Positioning System.

1. Introduction

Plate locking on the subduction thrust fault is the main source of deformation of an overriding continental margin during the interseismic period in the earthquake cycle at a convergent plate boundary. From the viewpoint of earthquake disaster mitigation, it is vital to understand the current state of plate locking as well as its lateral and downdip extents. The Nankai subduction zone of southwest Japan (Fig. 1) provides one of the best-studied examples of an earthquake cycle at the subduction zone because of the short recurrence time of great interplate earthquakes (100–150 years) and a well-recorded history of geodetic and seismological observations covering nearly one earthquake cycle. Interseismic crustal deformation in southwest Japan after the most recent events, the 1944 Tonankai ($M = 8.0$) and the 1946 Nankai ($M = 8.2$) earthquakes, has been dominated by interaction with the Philippine Sea plate that subducts beneath the southwest Japan arc at the Nankai Trough (Sagiya and Thatcher, 1999; Miyazaki and Heki, 2001).

In recent years, the Global Positioning System (GPS), which facilitates precise relative positioning, has enabled us to detect three-dimensional (3-D) crustal deformation with higher accuracy and over a shorter time period than those undertaken by conventional geodetic surveys. The nationwide continuous GPS array operated by the Geographical Survey Institute of Japan since 1994, now called GEONET (GPS Earth Observation Network) (Hatanaka *et al.*, 2003), has made a great contribution to crustal deformation studies in Japan, especially in areas of secular tectonic strain accumulation, coseismic rebound and postseismic transient and aseismic strain release due to slow fault slips (see summary by Sagiya, 2004). Moreover campaign GPS measurements focused on a specific area and time period have played a supplementary role to that of the GEONET. For example, combining crustal velocities from dense campaign GPS measurements with those from the GEONET, Tabei *et al.* (2002) showed that oblique subduction of the Philippine Sea plate at the Nankai Trough has formed a mobile forearc block that is moving slowly parallel to the southwest Japan arc. The mobile forearc block may be a characteristic common to the modern oblique subduction zones worldwide (McCaffrey, 1996). Therefore, it should be taken into consideration when interseismic crustal deformation in the oblique subduction zone is modeled, along with crustal shortening in the direction of plate convergence (Wang *et al.*, 2003).

Many previous studies have dealt solely with horizontal deformation because of its larger magnitude of signal than the vertical deformation and a lower accuracy of the vertical component in GPS solutions. However, longer observa-

tion periods together with recent advances in GPS receiver hardware and data analysis techniques are making it possible to discuss vertical deformation derived from GPS observations. For example, Suwa *et al*. (2006) estimated the distribution of interplate locking at the Japan Trench by inverting 3-D GPS velocity data obtained in northeast Japan over a five-year period. A similar method may be effective if applied to other subduction zones.

In this study we used both horizontal and vertical velocity fields of GEONET to model interseismic crustal deformation of the Nankai subduction zone. We demonstrate that the horizontal and vertical velocity fields are largely affected by plate locking at different depths, providing us with independent tectonic information. The main aim of this study was to estimate, through inversion analyses, the distribution of plate locking on the subduction fault, taking into consideration the existence of the mobile forearc block.

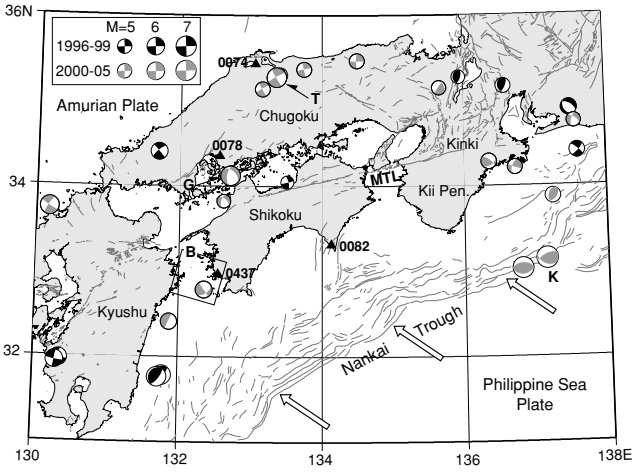

Fig. 1. Seismotectonic map of southwest Japan. Focal mechanism data of shallow earthquakes ($M > 5.0$ and $D < 60$ km) that occurred in 1997–2005 are taken from the broadband seismograph network (F-net) catalog of the National Research Institute for Earth Science and Disaster Prevention (http://www.fnet.bosai.go.jp/), and the data of 1996 are taken from the global CMT catalog of Harvard University (http://www.globalcmt.org/CMTsearch.html). Symbols "T", "G", and "K" denote the western Tottori earthquake ($M = 7.3$, $D = 11$ km) of October 6, 2000, the Geiyo earthquake ($M = 6.7$, $D = 51$ km) of March 24, 2001, and the earthquake off the Kii Peninsula ($M = 7.4$, $D = 44$ km) of September 5, 2004, respectively. Symbol "B" indicates the approximate source region of two slow thrust slip events beneath the Bungo channel in 1997 and 2003 (Hirose *et al*., 1999; Ozawa *et al*., 2004). Solid triangles with four-digit station codes indicate the locations of the continuous GPS stations of the GEONET for which coordinate time series are shown in Fig. 2. MTL: the Median Tectonic Line.

2. Data

2.1 GPS coordinate time series

Figure 1 shows the focal mechanisms of major shallow earthquakes ($M > 5.0$ and $D < 60$ km) in southwest Japan that occurred during the period 1996–2005. The most significant inland events are the Tottori earthquake of October 6, 2000 ($M = 7.3$ and $D = 11$ km, denoted by symbol "T" in Fig. 1) and the Geiyo earthquake of March 24, 2001 ($M = 6.7$ and $D = 51$ km, denoted by "G"). Seismic activity near the Nankai Trough is not necessarily high compared with the occurrence of moderate earthquakes in the surrounding region. The exception is the occurrence of the earthquake off the Kii Peninsula on September 5, 2004 ($M = 7.4$ and $D = 44$ km, denoted by "K") that was accompanied with a remarkable foreshock. Another notable feature is the occurrence of slow thrust slip events beneath the Bungo channel between Shikoku and Kyushu, whose source region is indicated by the symbol "B". On March 1997, coordinate time series at the GEONET stations in southwestern Shikoku began to deviate from the linear trends. The abnormal changes continued for about 300 days and amounted to a maximum of about 23 mm. Hirose *et al*. (1999) estimated that a slow thrust slip with a maximum of 18 cm occurred on the plate boundary and that the released seismic moment ultimately corresponded to that of an earthquake of $M_w = 6.6$. A similar event recurred there in 2004 (Ozawa *et al*., 2004).

We selected four GEONET stations to examine the site displacements. Station locations are indicated in Fig. 1, and the coordinate time series is shown in Fig. 2. Also shown in Fig. 2 are the time epochs of the instrumental renewals of the GPS receiver antennas to a different type; this was undertaken at all stations in 2002–2003. Stations 0074 and 0078 are located near the epicenters of the Tottori and Geiyo earthquakes, respectively. Their coordinate time series show nearly linear trends until the occurrence of the earthquakes. While coseismic jumps are recognized in the horizontal components, the effect on the vertical component is not clear because of large amplitudes of annual variation and daily scatters in addition to the small amplitude of the coseismic signal. However, the vertical component was greatly affected by the instrumental renewal. This effect is recognized as a jump in the time series and, possibly, a slight decrease of amplitudes of the annual variation and daily scatters. The coordinate time series of station 0437 shows transient motion in 1997 and 2003–2004 that synchronized with the occurrence of the slow thrust slip events. Station 0082 is located at some distance from the major earthquake sources, and its horizontal components show nearly linear trends with time except at the time epoch of the instrumental renewal. However, the time series of the vertical component seems to include a fluctuation of the trend behind the large annual variation in amplitude, though its origin is unknown.

2.2 Velocity data

As shown in Fig. 2, the GPS coordinate time series over nearly 10 years are not necessarily linear with time and are sometimes affected by seismic activity and the instrumental renewals. There is also a trend for change from an unknown origin, especially in the vertical component. In the Shikoku and Chugoku districts, the above effects were mostly concentrated in 2000 through 2003. To estimate linear site velocities, one needs to correct all factors that affected the time series or to select a specific time duration that was free from the above effects. In this paper we adopted the latter approach. We used crustal velocities from GEONET averaged over a period of 3.78 years from March 1996 to December 1999 under an improved analysis strategy (Hatanaka *et al*., 2003). Since the crustal activities in this period can be considered to be fairly moderate compared with those in subsequent years, this period may

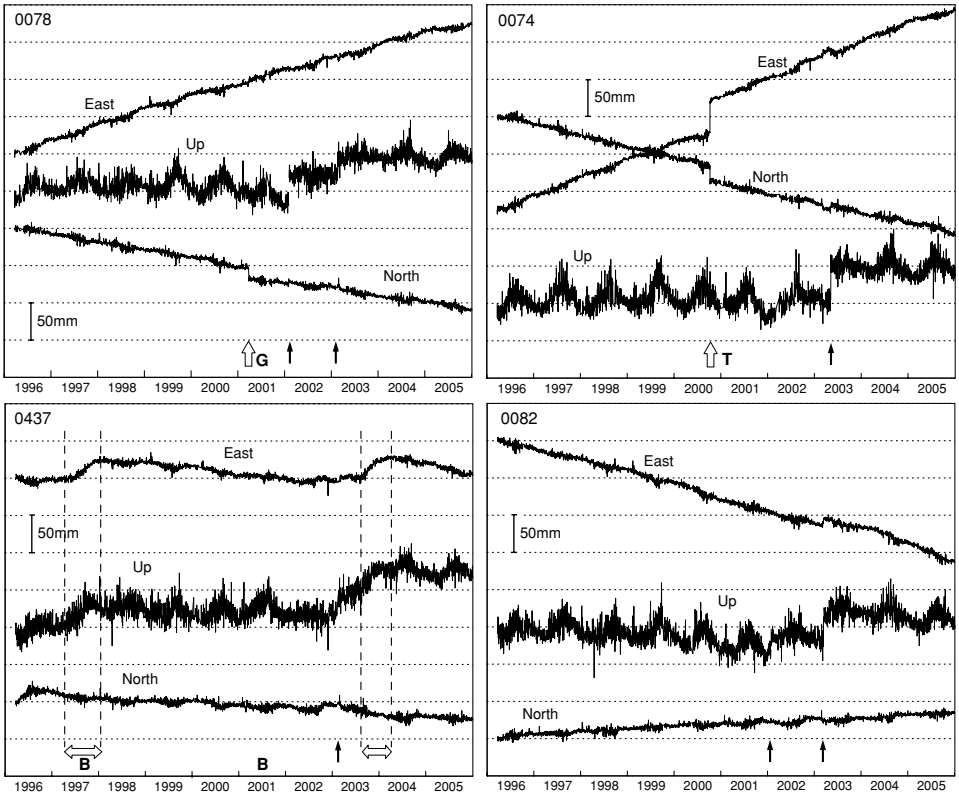

Fig. 2. Coordinate time series of four continuous GPS stations of the GEONET in the International Terrestrial Reference Frame. Thin solid arrows indicate the time epoch for instrumental renewal to a different type of the GPS receiver antenna. Thick open arrows accompanied by the symbols "T", "G", and "B" indicate the occurrence of the western Tottori earthquake ($M = 7.3$ and $D = 11$ km), the Geiyo earthquake ($M = 6.4$ and $D = 51$ km), and two slow thrust slip events beneath the Bungo channel, respectively. Refer to Fig. 1 for the locations of the GPS stations and the earthquakes.

be suitable for discussing quasi-stationary tectonic movements. One exceptional activity in this period was the occurrence of the slow slip event beneath the Bungo channel in 1997. Therefore, data obtained in 1997 in southwestern Shikoku were excluded from velocity estimations.

The original velocity fields are defined in the International Terrestrial Reference Frame (ITRF) 97. First, we changed the reference frame from ITRF to the Eurasian-fixed frame using the no-net-rotation NUVEL-1A plate model (DeMets *et al.*, 1994). Next, we converted to the Amurian-fixed frame using the Euler vector of the Amurian–Eurasian relative motion (Heki *et al.*, 1999). Sella *et al.* (2002) recently proposed a global plate model based on the space geodetic data in the period of 1993–2000, which included a direct conversion from ITRF to the Amurian-fixed frame. If we follow Sella *et al.* (2002), the north component of the horizontal velocity in the Shikoku district is estimated to be about 3 mm/yr smaller, while the difference in the east component is negligible. As we note later in Section 4, we use the Philippine Sea–Amurian Euler vector determined by Miyazaki and Heki (2001) to evaluate relative plate motion along the Nankai Trough. The Euler vector for the same plate pair defined by Sella *et al.* (2002) predicts an about 3 mm/yr smaller convergence rate in the north component at the Nankai Trough. We do not believe that the different realizations of the Amurian-fixed frame by DeMets *et al.* (1994) and Heki *et al.* (1999) or by Sella *et al.* (2002) have any critical effect on the inversion analyses in Section 4 because Sella *et al.* (2002) give a smaller convergence rate at the plate boundary, but equally smaller displacement rates on the overriding plate margin.

The horizontal velocity field with respect to the Amurian plate is shown in Fig. 3. The most significant feature is crustal shortening in the direction of convergence of the Philippine Sea plate. This can be interpreted as compressional elastic deformation caused by strong plate locking at the interseismic stage of the earthquake cycle at the Nankai Trough (Mazzotti *et al.*, 2000; Miyazaki and Heki, 2001; Aoki and Scholz, 2003a; Ito and Hashimoto, 2004). While most of the accumulated strain will be released at the time of the next great interplate earthquake, oblique subduction of the Philippine Sea plate is causing a small but permanent lateral movement of the forearc block along the arc-parallel strike-slip fault, the Median Tectonic Line (MTL). Tabei *et al.* (2002) conducted dense GPS traverse surveys across the MTL and showed that the residual velocity profile across the MTL, after removing elastic deformation caused by the subduction of the Philippine Sea plate, could be modeled by the locking of the shallower portion of the MTL fault plane and aseismic steady slip at depth at a rate of about 5 mm/yr. The slip rate derived from the dense GPS traverse surveys is in good accordance with the geological one in the Quaternary, 5–9 mm/yr (Tsutsumi and Okada, 1996).

Vertical deformations derived from GPS observations are height changes on the earth ellipsoid. In GEONET data processing, coordinates and velocities at all stations are ultimately referred to those at Tsukuba (36.1057°N, 140.0875°E), one of the International Global Navigation

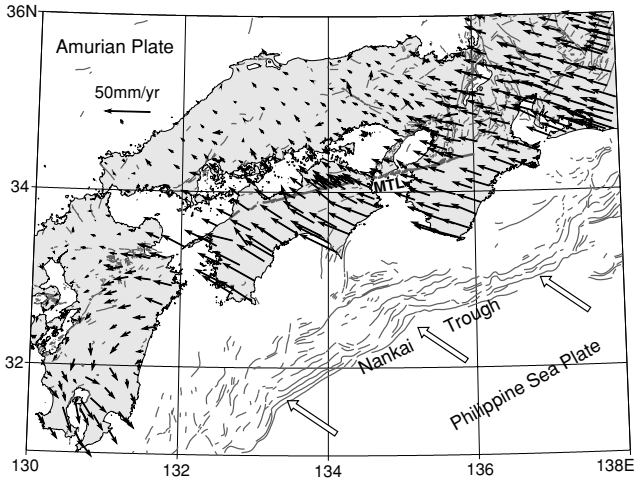

Fig. 3. Horizontal crustal velocity field of southwest Japan obtained from the nationwide continuous GPS array during the period March 1996 to December 1999 (Hatanaka *et al*., 2003). All velocities are plotted with respect to the Amurian plate.

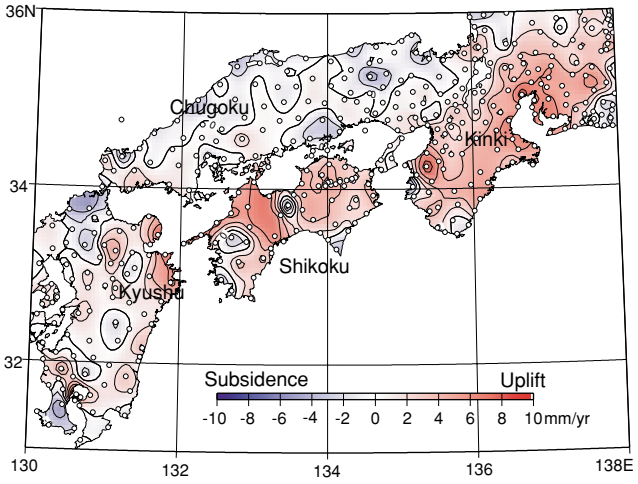

Fig. 4. Vertical crustal velocity field of southwest Japan obtained from the nationwide continuous GPS array during the period March 1996 to December 1999 (Hatanaka *et al*., 2003). The velocity field is adjusted so that the average of the site velocities in the Chugoku district equals zero.

Satellite System Service (IGS) stations. In the original velocity fields, about 92% of the 1002 stations in Japan show subsidence with a mean velocity of 4.7 mm/yr. We think that the original vertical velocity field contains a systematic bias originating from a bias probably existing in the velocity of Tsukuba in ITRF97. The vertical velocity at the Tsukuba IGS station has been estimated to be a subsidence of 4.4 mm/yr based on ITRF97, which is comparable to the mean subsidence rate over Japan, but it decreases to 0.6 mm/yr when the reference frame is changed to ITRF2000. Thus, it is difficult to establish a reliable absolute vertical datum. Murakami and Ozawa (2004) calculated vertical velocities of the GEONET stations and proposed a realistic solution such that the mean vertical velocity over the whole of Japan is set to zero. However, this assumption seems somewhat optimistic because the distributions of uplift and subsidence in a subduction zone, such as the Japanese Islands, is highly dependent on the station locations relative to the deformation source.

In this study, we adopted a more realistic vertical datum, assuming that crustal deformation is expected to be negligible in a region located far from plate boundaries or other deformation sources. The Chugoku district may be the best option as a temporary vertical datum for southwest Japan because it is distant from the plate boundaries, and no significant crustal activities have occurred in or around it during the period of velocity estimation, as shown in Fig. 1. We adjusted the vertical velocity field so that the mean velocity at about 80 stations in the Chugoku district, with a subsidence of 4.9 mm/yr, equaled zero.

The adjusted vertical velocity field is shown in Fig. 4. While the southern tips of the Shikoku and Kinki districts show a subsidence of 2–4 mm/yr, uplift up to 5–6 mm/yr is clear behind the subsidence area. This pattern can be interpreted as a bending of the overriding plate dragged along with the subducting Philippine Sea plate.

2.3 Error estimates

The original velocity fields processed under the improved analysis strategy had small estimation errors, with the medians for all stations being 0.05, 0.06, and 0.36 mm/yr for the east, north, and vertical components, respectively, when annual and semi-annual variations were introduced, but the errors of the reference site were not taken into consideration (Hatanaka *et al*., 2003). For a coordinate time series of 3 years processed under the previous analysis strategy, Miyazaki and Heki (2001) adopted mean velocity errors of 0.6 and 0.5 mm/yr for the east and north components, respectively, by introducing flicker noise in addition to white noise. Aoki and Scholz (2003b) combined GPS vertical velocities averaged over 3.78 years from 1996–1999 with those from the yearly mean tide gage data obtained in 1974–1999. Assuming that the tide gage data provided an absolute vertical datum, they adjusted the reference frame of the GPS velocities to fit the tide gage velocity field and showed that the precision of the vertical velocities is generally better than 2 mm/yr.

Here we adopted errors of 0.6 and 0.5 mm/yr for the east and north components, respectively, following Miyazaki and Heki (2001) though they do seem to be conservative for the revised solutions. Moreover, we assigned an error of 1.8 mm/yr for the vertical component, which is about three times larger than the horizontal ones, since it is empirically well known that the standard deviation of the vertical component in the GPS time series is a few times larger than that of the horizontal. The above errors do not contain frame-origin errors that arise when the velocity field is converted to that relative to a specific plate, which have been predicted to be as small as 1 mm/yr in southwest Japan (Heki *et al*., 1999).

2.4 Comparison of vertical velocities

We compare the vertical velocities with those derived from longer duration data. Murakami and Ozawa (2004) calculated vertical velocities from continuous GEONET data in 1996–2003, a few years longer than the data pe-

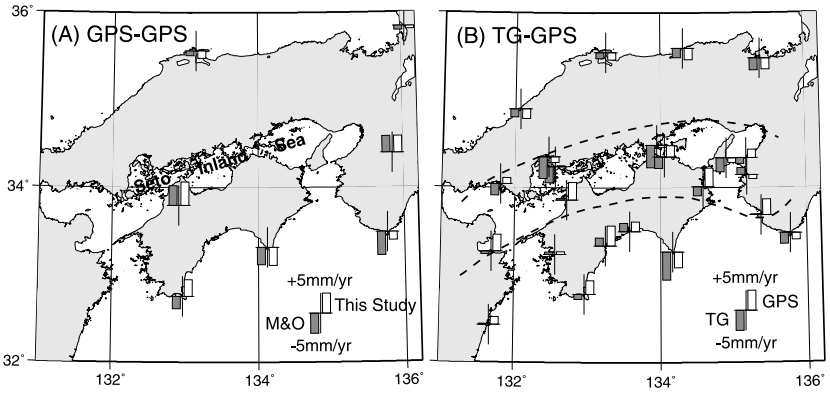

Fig. 5. Comparison of the vertical velocities of Fig. 2 with those derived from longer time series data. (A) Comparison with the velocities derived from daily coordinates of the GEONET in the period of 1996 to 2003 (Murakami and Ozawa, 2004). (B) Comparison with the velocities from monthly tide gage data for the 32–50 years up to 2004 (Coastal Movements Data Center, http://cais.gsi.go.jp/cmdc/centerindex.html). GPS velocities expected at the tide gage stations are calculated by the interpolation of the velocity field of Fig. 4. The inland sea region that is partitioned by two broken lines shows an inconsistency between the two kinds of velocities.

riod adopted in this study. Horizontal velocities were not derived. They adjusted the mean velocity over the whole of Japan, a subsidence of 3.3 mm/yr, to zero. Figure 5(A) shows velocity comparisons at the same GPS stations for which velocity values are explicitly given in their paper. Despite the different definition of the vertical datum, two kinds of velocities are consistent within 0.9 mm/yr at five stations—excepting two at the southwestern tip of the Shikoku and the southern tip of the Kinki districts.

Figure 5(B) shows a comparison with the vertical velocities derived from monthly mean tide gage data obtained over a 32- to 50-year period up to 2004, where the GPS velocity field of Fig. 4 is interpolated to give predictions at the locations of the tide gage stations. In this comparison, velocities from 23 tide gage stations are used, of which 15 are operated by the Japan Meteorological Agency, four by the Geographical Survey Institute, and four by the Japan Maritime Agency (data obtained from Coastal Movements Data Center). At four stations along the northern coast of the Chugoku district, two kinds of velocities show good consistency, within 0.6 mm/yr. In the southern part of the region, they are still compatible with each other, except at the southwestern tip of the Shikoku district. In contrast, in the Seto Inland Sea region that is partitioned by two broken lines, there is some inconsistency between the two kinds of velocities. Though we do not know what factor caused this difference, we speculate that it may have originated from the large difference in data length because the two GPS velocities are consistent with each other, even in the inland region, as shown in Fig. 5(A).

In the GPS vertical velocity field that was combined with the long-term tide gage data by Aoki and Scholz (2003b), fitness between the GPS and tide gage velocities in the Seto Inland Sea region was not clear. This is because these researchers used only tide gage data from the Geographical Survey Institute, and thus only three stations were located in the region in Fig. 5.

GPS vertical velocity fields show small but systematic subsidence along the northern coast of the Chugoku and Kinki districts. This seems to be inconsistent with the assumption of a stable Chugoku district that expects negligible motion far from the plate boundaries. However, it is also true that the vertical velocity field in the Chugoku district has an undulation of uplift and subsidence with a small amplitude and a zero mean. If we adjust the GPS vertical datum to fix the velocities along the northern coast of the Chugoku district to zero, agreements with the velocities from longer GPS data and with the long-term tide gage velocities will be degraded, and the inconsistency recognized in the Seto Inland Sea region will be enlarged.

3. Forward Estimation of Plate Locking at Depth

The downdip extent of the seismogenic zone at the Nankai Trough has been well reflected by a thermal model (Hyndman *et al.*, 1995). Based on this model, Miyazaki and Heki (2001) inferred that the plate boundary is fully locked to a depth of 25 km, locking strength decreases linearly with depth in the transition zone of 25–35 km, and there is no plate interaction below 35 km. These conditions have been used for other forward models of elastic deformation of the overriding plate caused by subduction of the Philippine Sea plate (e.g. Tabei *et al.*, 2002). Here, we demonstrate—using a simplified subduction fault model—that a trench-normal profile of the vertical velocity field is a good indicator of the plate locking in the transition zone.

Figure 6 shows the forward calculated velocity fields on the overriding plate along the trench-normal line. We assume a seismogenic subduction fault with a dip-angle of 10° and a length of 400 km parallel to the trench axis. The fault plane was divided into four segments according to the depth range (5–15 km, 15–25 km, 25–30 km, and 30–35 km). Slip deficit (or back slip) in the dip-slip component was applied on each fault segment. The slip deficit was postulated to be constant for each fault segment, while its rate varied according to the plate locking ratio, which was defined as the ratio of the slip-deficit rate to the plate convergence rate. Full plate locking (ratio 1.0) equals a convergence rate of 55 mm/yr in this model. Plate locking in the main seismogenic zone at depths of 5–25 km and in the deeper region below 35 km was assumed to be full and null, respectively. For the transition zone at depths of 25–30 km and 30–35 km, three different combinations of plate locking ra-

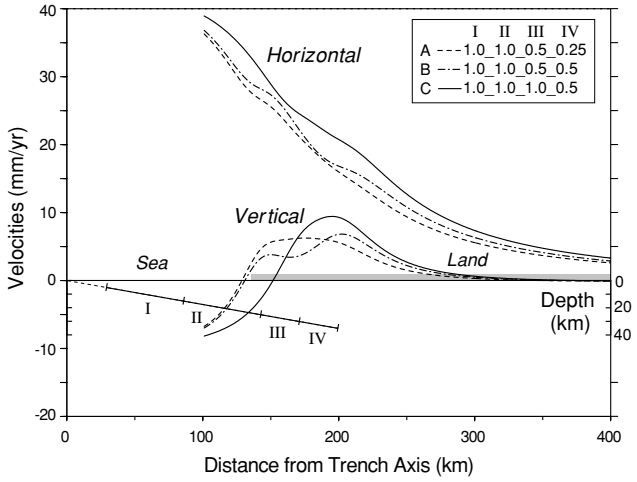

Fig. 6. Forward calculated velocity fields on the overriding plate along the trench-normal line. Seismogenic subduction fault with a dip-angle of 10° is divided into four segments according to the depth range (I: 5–15 km, II: 15–25 km, III: 25–30 km, and IV: 30–35 km), and slip deficits in the dip-slip component are applied on the fault segments. Velocity profiles are calculated for three different combinations of plate locking ratio (A, B, and C), as shown in the inset of the figure. Full plate locking (ratio of 1.0) equals 55 mm/yr in these calculations. Fault length is assumed to be 400 km parallel to the trench axis.

tio were assumed, as shown in the inset of Fig. 6. We calculated the surface deformations of the overriding plate by means of dislocation theory in an elastic half-space (Okada, 1985).

It is clear from Fig. 6 that the horizontal velocity field is not greatly affected by the change in the plate locking ratio in the transition zone. Though the rate itself increases slightly with an increasing ratio of locking in the transition zone, the general pattern of the horizontal deformation is conserved. This means that the horizontal velocity field is mainly dominated by strong locking in the main seismogenic zone at a depth of 5–25 km. By contrast, the vertical velocity field shows drastic changes in both rate and sense with an increasing ratio of locking in the transition zone. In particular there is a significant difference in the deformation pattern between profiles B and C in Fig. 6, indicating that the upper part of the transition zone at a depth of 25–30 km has a large effect on the surface vertical deformation.

The above forward model suggests that the horizontal and vertical velocity fields play supplementary roles to each other in the estimation of plate locking. The horizontal velocity field chiefly reflects strong plate locking in the main seismogenic zone offshore, but its general pattern is not greatly affected by the deep plate locking below the observed area. On the other hand, the vertical velocity field is more dependent on the latter.

4. Inversion Analysis of Fault Slip Deficit and Forearc Block Motion

4.1 Method

We made inversion analyses with *a priori* information using both horizontal and vertical velocity fields. See the appendix of Miyazaki and Heki (2001) for a mathematical description on this method.

Interseismic deformation is modeled by slip deficits on 21 fault planes at the plate interface given by Sagiya and Thatcher (1999) (see Fig. 7(D) for configuration), where uniform slip deficit is assumed on each fault segment. Additionally, we take into consideration a permanent lateral movement of the forearc block along the MTL. This can be modeled by superposing two different modes of movement (Matsu'ura *et al.*, 1986): one is the rigid motion of the forearc block without internal deformation, while the other is a marginal elastic deformation due to strike-slip deficits in the opposite sense on the upper locking zone of the MTL fault plane. The depth of the upper locking zone was fixed at 15 km based on the forward modeling results derived from dense GPS traverse surveys (Tabei *et al.*, 2002). Here, vertical movement of the MTL was not considered because the vertical slip rate estimated from geological surveys is much smaller (about one tenth) than the horizontal one (Research Group for Active Faults of Japan, 1991). A recent seismic reflection profiling in eastern Shikoku (Kawamura *et al.*, 2003) reveals a northward dipping fault plane of the MTL at a dip-angle of about 45° from the surface to a depth of about 7 km and at a shallower angle below to a depth of about 12 km. In western Shikoku, however, there is no direct information on the subsurface structure of the MTL, and the GPS station coverage becomes poorer. We divided the MTL into four segments of lengths 49–64 km, shown as M1 to M4 in Fig. 7(D), and assumed that each fault plane is inclined northward at a constant dip-angle through four segments from east to west.

In the inversion analyses, we used GPS velocities only in the Chugoku and Shikoku districts, roughly between 132° and 135° east longitude, to prevent crustal deformations resulting from other major tectonic origins. For example, it has become clear that horizontal GPS velocities in the Kinki district are affected by the collision of the southwest and northeast Japan arcs (Miyazaki and Heki, 2001). Moreover, counter-clockwise rotation of the velocity vectors in the Kyushu district (Fig. 3) strongly suggests the existence of other deformation sources in or west of Kyushu. The velocity data used for the inversion analyses are those obtained at a total of 121 GPS stations, 40 on the northern side of the MTL and 81 on the southern.

Since the GPS velocities have been obtained for only one side of the Nankai Trough, inversion analyses may result in unstable estimates or a degradation of the resolution. To stabilize the solutions, we imposed *a priori* information on unknown parameters. As for the plate interface, the initial direction of the slip deficit was chosen to coincide with that of the convergence vector of the Philippine Sea plate against the Amurian plate. The initial rate of slip deficit is the product of the convergence rate of the Philippine Sea plate and the depth-dependent locking ratio. The *a priori* information on the locking ratio is specifically expressed as full locking of the fault segments at a depth 5–25 km, 75% at 25–30 km, 50% at 25–35 km, 25% at 30–35 km, and no interaction below 35 km; shown by black solid dots in Fig. 8(A). As for the lateral movement of the forearc, an initial rate of 5 mm/yr was given to the rigid block motion parallel to the strike of MTL, and a left-lateral strike-slip with an initial rate of 5 mm/yr was given for the upper fault zone of the MTL to realize the locking of the fault.

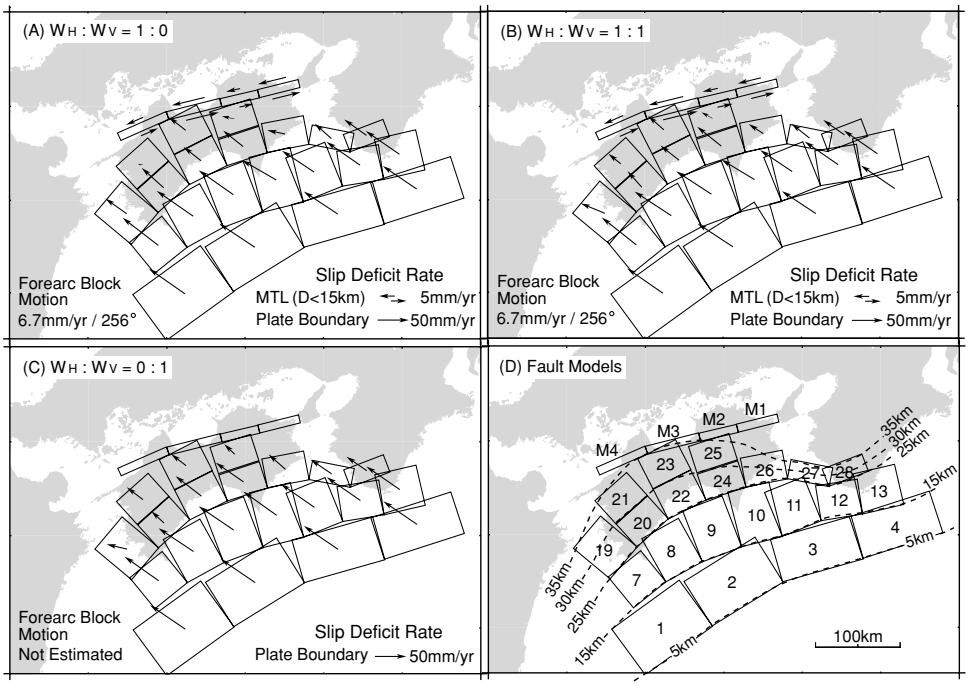

Fig. 7. Inversely estimated slip deficit vectors by applying different data weights for horizontal and vertical velocities. (A): Only horizontal velocity data were used to estimate slip deficit rates at the Nankai Trough plate boundary, slip deficit rates in the shallower portion of the MTL, and the rate of lateral movement of the forearc block. (B): Both horizontal and vertical velocity data were used with equal weights. (C): Only vertical velocity data were used. Lateral motions of the MTL and forearc block were not considered. (D): Horizontal projection of rectangular fault planes used in the analyses. Fault geometry and attached number at the Nankai Trough plate boundary come from Sagiya and Thatcher (1999). The MTL was modeled by four segments, M1 to M4, with northward dipping fault planes.

We imposed an *a priori* standard deviation of 1 mm/yr on each of the strike and dip components of the slip deficit at the main seismogenic zone of the Nankai Trough at a depth of 5–25 km (fault segments 1–4 and 7–13 in Fig. 7(D)). The small standard deviation would tightly constrain the estimates to the initial values. In contrast, we imposed a three times larger standard deviation of 3 mm/yr on the slip deficit at the transition zone at a depth of 25–35 km, considering the larger ambiguity of the slip distribution there. Similarly, we imposed a value of 3 mm/yr on the strike-slip deficits of four segments of the MTL and the rate of rigid block motion.

The inversion analyses with *a priori* information are summarized as minimizing the following function:

$$s(\mathbf{m}) = (\mathbf{d}-G\mathbf{m})^T \Sigma_{\mathrm{d}}^{-1}(\mathbf{d}-G\mathbf{m})+\beta^2(\mathbf{p}-\mathbf{m})^T \Sigma_{\mathrm{p}}^{-1}(\mathbf{p}-\mathbf{m}),$$

where **m**, **d**, and **p** are the vectors of the unknown model parameters, observed data, and *a priori* information, respectively. G is a data kernel that relates the slip on the fault segments with the surface displacements (Okada, 1985), and Σ_{d} and Σ_{p} are the covariance matrices of the observed data and *a priori* information, respectively. β^2 is a scaling factor that characterizes the relative weight of *a priori* information to the data, which is optimized to minimize the Bayesian information criterion (ABIC) value.

As described in Section 2.3, velocity errors of 0.6, 0.5, and 1.8 mm/yr were adopted for the east, north, and vertical components, respectively. One important question arising when three components of the velocity are simultaneously used is how large a weight should be assigned to each component. Generally speaking, the error of the vertical component in a GPS solution is roughly a few times larger than that for the horizontal. Therefore, it is natural to assign a larger weight to the horizontal velocities. As pointed out in Section 3, however, horizontal and vertical velocities are largely affected by plate locking at different depths, providing us with independent tectonic information. From this point of view, it is also reasonable to assign comparable weights to the horizontal and vertical components. Here, we carried out inversion analyses for the following five cases: (1) only horizontal velocity data were used, (2) a data weight ratio of 9:1 was assigned to the horizontal and vertical velocity data, (3) a weight ratio of 4:1 was assigned, (4) equal weights were adopted, and (5) only vertical velocity data were used. The error of the vertical component was intentionally reduced to 1.2 mm/yr in case (3) and 0.6 mm/yr in case (4). In the last case (5), a lateral movement of the forearc block along the MTL was excluded from the estimation.

4.2 Results

The parameters to be simultaneously determined were the slip deficit vectors on the 21 fault planes at the plate interface, the strike-slip deficit rates on the upper zone of the four segments of the MTL, and the rate of rigid lateral motion of the forearc block. The optimum dip-angle of the MTL fault plane was investigated in the preliminary analysis for case (1) using only the horizontal velocity data. This was because the fault motion of the MTL was originally a strike-slip and the dip-angle of the MTL fault plane affects the horizontal velocity profile across the MTL, while there was no significant effect on the vertical velocities. Varying the dip-angle of the MTL with a step of 10°, we carried out

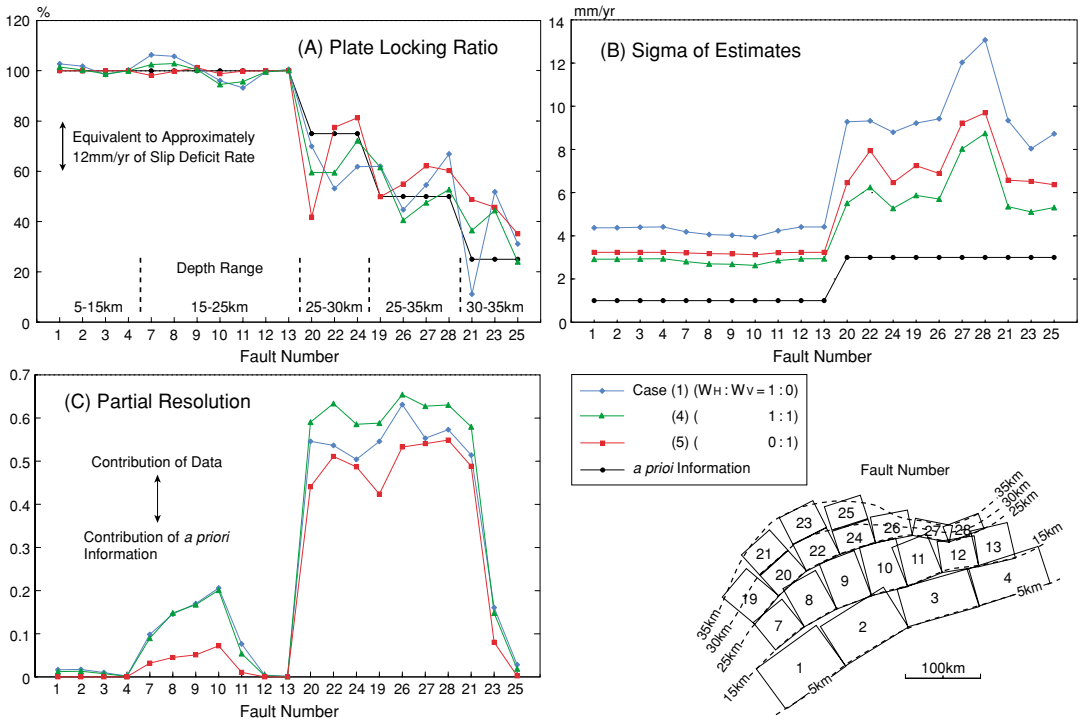

Fig. 8. Inversely estimated (A) plate locking ratio, (B) standard deviation of the estimated slip deficit rate, and (C) normalized partial resolution of data for the fault segments at the Nankai Trough plate boundary. Three cases with different data weights for horizontal and vertical velocities are shown. Black solid circles indicate the *a priori* information (initial values) of the inversion analyses.

inversion analyses for case (1). The most likely model with the minimum ABIC value was obtained when the dip-angle of the MTL was predefined as 50°. This result is consistent with the dip-angle revealed by a seismic reflection profiling survey (45°) (Kawamura *et al.*, 2003) and the estimate from dense GPS traverse surveys (35°) (Tabei *et al.*, 2002). Thus, for the analyses for cases (2) to (5) we fixed the dip-angle of the MTL to 50°.

Inversion results for cases (1), (4), and (5) are illustrated in Fig. 7(A), (B), and (C), respectively. Moreover the plate locking ratio at the Nankai Trough is shown in Fig. 8(A), which is defined as the ratio of the estimated slip deficit to the predicted relative velocity between two plates (Miyazaki and Heki, 2001). General features of the slip deficit distribution are similar between these three cases. The slip deficit rate is as large as 65 mm/yr, almost full locking, in the main seismogenic zone at a depth of 5–25 km (fault segments 1–4 and 7–13) in a direction nearly parallel to the plate convergence. However, the rate decreases and the direction shows a small variation with increasing depth. In Fig. 7(A) and (B) where the horizontal velocity field was used, the rate of lateral motion of the forearc block was estimated to be 6.7 mm/yr parallel to the strike of MTL and strike-slip deficits on the upper zone of four segments of the MTL were estimated to be 4.6–10.8 mm/yr with a mean rate of 7.6 mm/yr.

Standard deviations of the estimated slip deficit rates at the plate interface are shown in Fig. 8(B). They are the smallest on the shallow seismogenic segments 1–4 and 7–13. This result can be expected because the smallest *a priori* standard deviation was imposed there to tightly constrain the estimates to the initial values, as described in Section 4.1. For the other fault segments, standard deviations are nearly twice as large as those at the shallow segments, except on segments 27 and 28. In most segments, the standard deviations of the estimates do not exceed the slip deficit rates. The best result is obtained for case (4), where equal weights were adopted for the horizontal and vertical components. The profile of the standard deviation for case (3), where a data weight of 4:1 was assigned, is close to that of case (4) (not shown in the figure). Standard deviations of the estimated slip deficit rates on the MTL fault plane were about 3 mm/yr in segments M2 and M3, and 5–6 mm/yr in M1 and M4.

The contribution of data and *a priori* information to the estimates was evaluated by comparing diagonal components of their partial resolution matrices. Figure 8(C) shows a normalized partial resolution of data, with the larger value indicating a larger contribution of data. The contribution of data to the estimates was negligible, and the results were mostly dependent on the *a priori* information in far shallower segments, 1–4, 12, and 13. On the other hand, the data had a larger contribution in segments just below the Shikoku district. The contributions of data were larger in the fault segments of MTL than in those at the plate boundary, about 82–95% in segments M2 and M3, and 64–83% in M1 and M4 (not shown in Fig. 8(C)).

Velocity residuals between the observations and the predictions from the slip deficit model were about 2.0–2.3 mm/yr in the root-mean-squares (rms), while the minimum rms was obtained in case (5), which uses only vertical velocity data. The rms values seem to largely depend on outliers among the original velocity data. When inspecting residuals of the horizontal velocity fields, 15 of 121 stations

showed residuals larger than 4 mm/yr, and nine showed residuals larger than 5 mm/yr. On the other hand, in the vertical velocity field, the residuals exceeded 4 mm/yr at six stations, and 5 mm/yr at just three. Except for those stations with possible outliers, the residuals are as small as 2 mm/yr in the rms, indicating a good fit to the model.

5. Discussion

Slip deficit rates of the upper zone of the MTL fault segments—4.6–10.8 mm/yr with a mean of 7.6 mm/yr, are comparable to the rate of the lateral motion of the forearc block—6.7 mm/yr, in the opposite direction. Taking into consideration errors resulting from velocity data and inversion analyses, the above result shows that the upper zone of the MTL fault plane is almost fully locked to a depth of 15 km. This is consistent with the geological observation that no creep motion is currently seen across the surface trace of the MTL (Tsutsumi and Okada, 1996). How far the forearc lateral motion extends and where and how it terminates are important problems to be resolved in the future. Crustal deformation fields over a wider area that show drastic changes from Shikoku to Kyushu (Fig. 3) will need to be dealt with.

Closely examining the distribution of the plate locking ratio in Fig. 8(A), we find that inversion analysis using only horizontal or vertical velocity data (case (1) or (5)) resulted in locally very different estimates at the specific fault segments, such as 20 and 21, even though two analyses started from the same *a priori* information. The difference between the two estimates is about 28% (18 mm/yr) and 38% (25 mm/yr) in segments 20 and 21, respectively, which exceeds the standard deviation of the estimate. On the other hand, the result for case (4), which was derived from a combination of horizontal and vertical data, gives intermediate estimates at those segments and, as a whole, a smoother distribution of plate locking. The advantages of combining horizontal and vertical data are more directly shown by the reduction of the standard deviations of the estimated parameters (Fig. 8(B)) and by the increase of the partial resolution of data (Fig. 8(C)). These improvements may have been attained by the increasing amount of data and the combination of different spatial resolutions of data that were expected from the different spatial patterns of horizontal and vertical deformations (Fig. 6).

How large a weight should be assigned to each component of the velocity data has not been clearly resolved. As for the standard deviations of the estimates, the smallest values were obtained in case (4), where equal weights were adopted for the horizontal and vertical data. The standard deviations in case (3), where a data weight of 4:1 was assigned, are similarly small. As for the partial resolution of data, the largest values are obtained in case (4), but the difference from the second best result for case (2) is negligible, where a data weight ratio of 9:1 was assigned. In a statistical sense, the best solution is obtained in case (4), but its superiority over the second best solution is small. However, it should be noted that giving equal weights to the horizontal and vertical data, as in case (4), resulted in the best solution for both the standard deviation and the partial resolution of data. This implies that horizontal and vertical velocity fields, which are largely affected by plate locking at different depths, provide us with independent tectonic information.

Estimated slip deficit rates (Figs. 7(A), (B), (C), and 8(A)) show nearly full locking of the seismogenic fault segments at a depth of 5–25 km at the interseismic stage. This result is common to most previous studies that dealt with GPS velocities for their inversion analyses (e.g. Mazzotti *et al.*, 2000; Miyazaki and Heki, 2001; Ito and Hashimoto, 2004), although the researchers adopted different data handling, inversion schemes, and geometries for the plate interface. By contrast, coseismic slip distribution at the 1944 Tonankai and 1946 Nankai earthquakes inverted from conventional geodetic data shows large spatial variation, not only in the downdip direction but also along the subduction margin (Sagiya and Thatcher, 1999; Ito and Hashimoto, 2004). The maximum coseismic slip zone is located southeastern off Shikoku, where the slip is estimated to be 11–13 m, but it is reduced to about 10 m when viscoelastic response is introduced to the asthenosphere (Ito and Hashimoto, 2004) or to about 6 m when shallow splay faults are introduced (Sagiya and Thatcher, 1999). Different spatial distribution patterns between the coseismic slip at the last great interplate earthquakes and the interseismic slip deficit at present is an important issue to be discussed in a future study because it may be closely related to the coseismic strain release at the time of the next great earthquake.

We have been interested in plate locking on fault segments 19–21 km below the western Shikoku because these segments overlap with or are located very near the source region of a slow thrust slip event. To remove abnormal surface displacements related to the slow event from velocity estimations, data obtained in 1997 in southwestern Shikoku were not used for the analyses (Hatanaka *et al.*, 2003). However, it is reasonable to expect that plate locking on these fault segments is somewhat different from those on other segments that are at the stage of steady-state strain accumulation. Unfortunately, it is not clear whether or not the estimated plate locking on segments 19–21 are reliable enough and stationary. We believe that the low estimates at segment 20 in case (5) and at segment 21 in case (1) may be artifacts, probably due to low spatial resolution, estimation errors, and outliers of velocity data nearby.

Plate locking ratios at the transition zone, on segments 19 and beyond, are generally larger than those predicted with earlier models. For example, Miyazaki and Heki (2001) assumed 75% for fault segments at the depth of 25–30 km, 50% for those at 25–35 km, and 25% for those at 30–35 km within the framework of a thermal model (Hyndman *et al.*, 1995). Our inversion results, especially when the vertical velocity data are used with the larger weights, tend to show larger estimates at the transition zone than previous assumptions.

Distribution of the plate locking at the transition zone may have a trade-off with the updip and downdip extents of the zone. In this study, we have fixed the upper and lower limits of the transition zone to 25 km and 35 km, respectively, throughout the plate boundary. On the other hand, Wang *et al.* (2003) introduced the concept of an effective transition zone in the Cascadia subduction zone; this claims

that plate locking weakens exponentially with the downdip distance and, therefore, the lower limit of the transition zone extends deeper but is not explicitly defined. The main purpose for introducing this model is to reproduce the surface deformation caused by the viscous flow in the mantle wedge at a time as long as 300 years after a great interplate earthquake. At the Nankai subduction zone, however, the viscous flow does not seem to have an important role in producing surface deformation because the recurrence time of the great interplate earthquake is much shorter, about 100–150 years. Nevertheless, future modeling should consider local variations in the depth range of the transition zone because lateral variation of the subduction process is seen in the Nankai region. The trough changes to a more southward strike and the plate convergence direction becomes more normal to the plate boundary off eastern Kyushu. At the same time, the dip-angle of the subducting plate becomes much steeper. The subduction effect of the steep slab off eastern Kyushu should be incorporated into future modeling, and different depth-dependences of the slip deficit distribution may thus be expected there.

6. Conclusions

We inverted 3-D GPS velocity data for southwest Japan to estimate interseismic slip deficits at the Nankai Trough plate interface, along with the partial locking of the shallower portion of the MTL fault plane and the permanent lateral movement of the forearc. We carried out inversion analyses with *a priori* information, varying data weights for the horizontal and vertical velocity data. Combining vertical with horizontal data led to the smooth distribution of plate locking, a reduction of the standard deviations of the estimated parameters, and an increase of the partial resolution of data. The best solutions were obtained when equal weights were assigned to horizontal and vertical data.

The inversion results show that the seismogenic subduction faults at a depth of 5–25 km are strongly locked. As for the transition zone at 25–35 km, plate locking is estimated to be slightly larger than that reported in previous studies, especially when vertical velocity data are given larger weights. The rate of lateral forearc movement and the slip deficit rates at the MTL fault plane are nearly comparable, in a reverse sense, to each other. Taking into consideration errors resulting from velocity data and inversion analyses, the shallower portion of the MTL may be strongly locked and stationary aseismic slip occurring in the deeper part.

Acknowledgments. We thank GSI for providing us crustal velocity data of the GEONET. The tide gage velocity data are obtained through the Coastal Movements Data Center. Critical reviews by S. Mazzotti, T. Sagiya (the editor), and an anonymous referee improved the quality of the paper. This work was partly supported by the Special Project for the Earthquake Disaster Mitigation in Urban Areas (2002–2007) from the Ministry of Education, Culture, Sports, Science and Technology.

References

Aoki. Y. and C. H. Scholz, Vertical deformation of the Japanese islands, 1996–1999, *J. Geophys. Res.*, **108**, doi:10.1029/2002JB002129, 2003a.

Aoki. Y. and C. H. Scholz, Interseismic deformation at the Nankai subduction zone and the Median Tectonic Line, southwest Japan, *J. Geophys. Res.*, **108**, doi:10.1029/2003JB002441, 2003b.

DeMets, C., R. G. Gordon, D. F. Argus, and S. Stein, Effect of recent revisions to the geomagnetic reversal time scale on estimates of current plate motions, *Geophys. Res. Lett.*, **21**, 2191–2194, 1994.

Hatanaka, Y., T. Iizuka, M. Sawada, A. Yamagiwa, Y. Kikuta, J. M. Johnson, and C. Rocken, Improvement of the analysis strategy of GEONET, *Bull. Geogr. Surv. Inst.*, **49**, 1–35, 2003.

Heki, K., S. Miyazaki, H. Takahashi, M. Kasahara, F. Kimata, S. Miura, N. F. Vasilenko, A. Ivashchenko, and K-D. An, The Amurian Plate motion and current kinematics in eastern Asia, *J. Geophys. Res.*, **104**, 29,147–29,155, 1999.

Hirose, H., K. Hirahara, F. Kimata, N. Fujii, and S. Miyazaki, A slow thrust slip event following the two 1996 Hyuganada earthquakes beneath the Bungo Channel, southwest Japan, *Geophys. Res. Lett.*, **26**, 3237–3240, 1999.

Hyndman, R. D., K. Wang, and M. Yamano, Thermal constraints on the seismogenic portion of the southwestern Japan subduction thrust, *J. Geophys. Res.*, **100**, 15,373–15,392, 1995.

Ito, T. and M. Hashimoto, Spatiotemporal distribution of interplate coupling in southwest Japan from inversion of geodetic data, *J. Geophys. Res.*, **109**, B02315, doi:10.1029/2002JB002358, 2004.

Kawamura, T., M. Onishi, E. Kurashimo, T. Ikawa, and T. Ito, Deep seismic reflection experiment using a dense receiver and sparse shot technique for imaging the deep structure of the Median Tectonic Line (MTL) in east Shikoku, Japan, *Earth Planets Space*, **55**, 549–557, 2003.

Matsu'ura, M., D. D. Jackson, and A. Chen, Dislocation model for aseismic crustal deformation at Holister, California, *J. Geophys. Res.*, **91**, 12,661–12,674, 1986.

Mazzotti, S., X. Le Pichon, P. Henry, and S. Miyazaki, Full interseismic locking of the Nankai and Japan-west Kurile subduction zones: An analysis of uniform elastic strain accumulation in Japan constrained by permanent GPS, *J. Geophys. Res.*, **105**, 13,159–13,177, 2000.

McCaffrey, R., Estimates of modern arc-parallel strain rates in fore arcs, *Geology*, **24**, 1139–1142, 1996.

Miyazaki, S. and K. Heki, Crustal velocity field of southwest Japan: Subduction and arc-arc collision, *J. Geophys. Res.*, **106**, 4305–4326, 2001.

Murakami, M. and S. Ozawa, Mapped vertical deformation field of Japan derived from continuous GPS measurements and its tectonic implications, *J. Seism. Soc. Jpn*, **57**, 209–231, 2004 (in Japanese).

Okada, Y., Surface deformation due to shear and tensile faults in a half-space, *Bull. Seism. Soc. Am.*, **75**, 1135–1154, 1985.

Ozawa, S., Y. Hatanaka, M. Kaidzu, M. Murakami, T. Imakiire, and Y. Ishigaki, Aseismic slip and low-frequency earthquakes in the Bungo channel, southwestern Japan, *Geophys. Res. Lett.*, **31**, L07609, doi:10.1029/2003GL019381, 2004.

Research Group for Active Faults of Japan, *Active Faults in Japan: Sheet Maps and Inventories*, 437pp, Univ. Tokyo Press, Tokyo, 1991 (in Japanese).

Sagiya, T., A decade of GEONET: 1994–2003—The continuous GPS observation in Japan and its impact on earthqauke studies—, *Earth Planets Space*, **56**, xxix-xli, 2004.

Sagiya, T. and W. Thatcher, Coseismic slip resolution along a plate boundary megathrust: The Nankai Trough, southwest Japan, *J. Geophys. Res.*, **104**, 1111–1129, 1999.

Sella, G. F., T. H. Dixon, and A. Mao, REVEL: A model for Recent plate velocities from space geodesy, *J. Geophys. Res.*, **107**, doi:10.1029/2000JB000033, 2002.

Suwa, Y., S. Miura, A. Hasegawa, T. Sato, and K. Tachibana, Interplate coupling beneath NE Japan inferred from three-dimensional displacement field, *J. Geophys. Res.*, **111**, B04402, doi:10.1029/2004JB003203, 2006.

Tabei, T., M. Hashimoto, S. Miyazaki, K. Hirahara, F. Kimata, T. Matsushima, T. Tanaka, Y. Eguchi, T. Takaya, Y. Hoso, F. Ohya, and T. Kato, Subsurface structure and faulting of the Median Tectonic Line, southwest Japan inferred from GPS velocity field, *Earth Planets Space*, **54**, 1065–1070, 2002.

Tsutsumi, H. and A. Okada, Segmentation and Holocene surface faulting on the Median Tectonic Line, southwest Japan, *J. Geophys. Res.*, **101**, 5855–5871, 1996.

Wang, K., R. Wells, S. Mazzotti, R. D. Hyndman, and T. Sagiya, A revised dislocation model of interseismic deformation of the Cascadia subduction zone, *J. Geophys. Res.*, **108**, 2026, doi:10.1029/2001JB001227, 2003.

T. Tabei (e-mail: tabei@kochi-u.ac.jp), M. Adachi, S. Miyazaki, T. Watanabe, and S. Kato